THE UNIVERSITY OF MICHIGAN

College of Engineering

Department of Mechanical Engineering

Cavitation and Multiphase Flow Laboratory

Report No. UMICH 03371-15-T

ON THE EFFECTS OF HEAT TRANSFER UPON COLLAPSING BUBBLES

(To be Submitted for Publication to
International Journal of Heat and Mass Transfer)

by

Terry Mitchell*

Frederick G. Hammitt**

Financial Support Provided by

National Science Foundation
Grant No. GK-13081

Research Associate (Formerly Doctoral Candidate)
Professor-In-Charge

January 1972

ABSTRACT

The effects upon spherically-symmetric bubble collapse of the various thermodynamic parameters including interfacial non-equilibrium boundary effects are examined numerically, for the case of cavitation or highly subcooled boiling bubbles. Pressures in the surrounding liquid as a function of time and distance are computed. It is shown that the value selected for the evaporation coefficient, not well known experimentally, has a very strong influence on collapse pressures and velocities. The thermal diffusivity of the bubble contents is also significant but somewhat less important. The effect of non-equilibrium temperature or pressure discontinuities at the interface were found negligible for the cases studied.

ACKNOWLEDGEMENTS

Financial support for this work was provided under NSF Grant GK-13081. The authors would also like to thank Mr. N. R. Bhatt and Miss Nancy J. Parsons for their assistance in the assembling and typing of the paper.

LIST OF FIGURES

LIST OF TABLES

NOMENCLATURE

Symbol	Description
C_v	Constant volume specific heat
C_p	Constant pressure specific heat
h_{fg}	Latent heat of evaporation
h_g	Saturated steam enthalpy
(J)	Work-energy conversion constant
k_f	Liquid thermal conductivity
$\frac{k}{k+1}$	Transport coefficient defined in Ref. 15
L_k	Transport coefficient defined in Ref. 15
m	Mass
p	Pressure
$p_{v_{sat}}(T)$	Saturation vapor pressure corresponding to temperature T
$\dot{q}$	Heat condition rate into bubble/unit area
R	Bubble radius
$\bar{R}$	Gas constant
r	radial coordinate
$T_{(\ )}$	Temperature of particular component (absolute)
T	Dimensionless total collapse time = 0.91468
$\bar{T}_g$	Average gas temperature over bubble volume (absolute)
T_{g_i}	Gas temperature at interface (absolute)
T_{L_i}	Liquid temperature at interface (absolute)
t	Time
U	Bubble wall velocity; total internal energy
u	Radial velocity
u_g	Saturated steam internal energy
v_L	Liquid specific volume
v	Gas specific volume
$\dot{w}$	Rate at which work is done on bubble contents per unit surface area
α	Evaporation (or condensation) coefficient

α_L	Liquid thermal diffusivity
α_g	Gas thermal diffusivity
δ	Polytropic exponent
γ_1	$T_\infty - T_{L_i}$
ε	$1 - \rho_v/\rho_L$
μ_L	Liquid viscosity
ρ	Density
σ	Surface tension
τ	Dimensionless time

Subscripts

g	Non-consensable gas + vapor
i	Non-condensable gas
L	Liquid
v	Vapor
∞	Value at large r
o	Initial value

Superscripts

$\dot{}$	Time derivative
$\tilde{}$	Dimensionless

I. INTRODUCTION

An accurate modelling of cavitation bubble collapse is contingent on knowledge of the role of a variety of individual effects. A major effect is that of asymmetry, treated elsewhere and including contributions of the present authors[1, 2]. Also, there are the effects of a number of mechanical and "thermodynamic" parameters to be examined even if the collapse remains spherical. In the first category there are, e.g., the effects of liquid surface tension, viscosity, and compressibility, and these effects have been examined (e.g., 3,4). In addition, other investigators have modelled spherical bubble collapses considering the individual effects of phase change, spatial temperature variation both inside and outside the bubble, the value of the evaporation coefficient, the thermal conductivity of the internal contents, interfacial discontinuities, and the presence of a non-condensable gas (e.g., 5-9, 20).

The aim of the present work is to "model", as realistically as possible, spherically-symmetric cavitation bubble collapse including all of the above parameters*.

II. ANALYSIS

The problem to be solved is that of a spherical bubble of initial radius R_o containing both non-condensable (and non-diffusing) gas and saturated vapor. The bubble is located in an infinite mass of incompressible liquid; initially its internal contents are in mechanical equilibrium (pressure and surface tension). The liquid and bubble are initially at temperature T_∞. The initial non-condensable gas partial pressure is p_{i_o}, while that of the vapor is $p_{v_o} = p_{v_{sat}}(T_\infty)$. At time zero the system pressure is increased instantaneously to p_∞ and the collapse ensues. For clarity, the adjective "non-condensable" will always be included when reference is made to only that component. The term "gas" in the subsequent text refers to noncondensable gas plus vapor.

---

*Portion of Ph. D. dissertation[2] of first author.

The additional assumptions made in developing the model for such collapses include:

1) Both non-condensable gas and vapor obey the perfect gas law. The bubble wall will be assumed to remain sufficiently smaller than the sonic velocity in the gas-vapor mixture throughout the calculation so that the vapor and non-condensable gas pressures may be assumed uniform throughout the bubble at any given time. Since in fact asymmetries will prevent the volume reduction ratio proceeding to very small values, this assumption is realistic.

2) The rate of condensation or evaporation at the interface is defined by the kinetic theory equation (Eq. (5)).

3) The heat conducted out into the liquid is equal to the sum of the latent heat component deposited on the wall by condensation and the heat conducted out from the bubble contents. This heat conducted out through the liquid results in the formation of a thin thermal boundary layer in the liquid which was assumed to be of parabolic temperature distribution. Such an assumption is reasonably valid as long as the bubble contents temperature increases monotonically, Once the bubble contents temperature starts to drop, e.g., during rebound, the assumed temperature profile shape is no longer valid. However, calculations were not continued into the rebound phase.

4) There is a thin but finite nonequilibrium region at the interface because of the continuing process of phase change there, which region contains both temperature and pressure discontinuities between the liquid and the vapor.

5) The temperature within the bubble does not remain uniform. In all previous cavitation bubble collpase analyses known to the authors, with the exception of Hickling's treatment of sonoluminescence[6], the contents of the bubble are assumed to be at uniform temperature at any given time. By assuming that the rate at which work is being

done on the bubble is constant over short time segments of the collapse and neglecting radiative and convective heat transfer, the temperature history can be treated as a classical heat conduction problem (over the same short time segments), i.e., that of a sphere with given initial temperature profile and known surface temperature.

Fig. 1(a) is a sketch of the bubble with surrounding liquid with the temperatures, pressures, and densities at the appropriate points labelled with the same symbols used in the equations which follow. Fig. 1(b) shows a typical temperature profile from the bubble center to the liquid far from the bubble at some time after the beginning of the calculation.

The details of the derivation of the governing equations are presented elsewhere [2], and acknowledgement is made to a number of previous related works [10-14]. The complete system of equations follows:

$$r^2 u = R^2 U = g(t) \tag{1}$$

$$u(R) = \epsilon \dot{R} - \frac{R \dot{\rho}_v}{3 \rho_L} \tag{2}$$

$$\left[\epsilon \ddot{R}R + 2\epsilon (\dot{R})^2 - \frac{2R\dot{R}\dot{\rho}_v}{\rho_L} - \frac{R^2 \ddot{\rho}_v}{3\rho_L}\right] \left(\frac{R}{r}\right) - \frac{1}{2}\left(\frac{R}{r}\right)^4 \cdot$$

$$\left(\epsilon \dot{R} - \frac{R\dot{\rho}_v}{3\rho_L}\right)^2 = \frac{1}{\rho_L}\left[p_L(r) - p_\infty\right] \tag{3}$$

$$\epsilon \ddot{R}R + 2\epsilon (\dot{R})^2 - \frac{2R\dot{R}\dot{\rho}_v}{\rho_L} - \frac{R^2 \ddot{\rho}_v}{3\rho_L} - \frac{1}{2} u(R)^2$$

$$= \frac{1}{\rho_L}(p_g(t) - p_\infty) - \frac{2\sigma}{\rho_L R} - \frac{4\mu_L}{\rho_L R} u(R) \tag{4}$$

$$\frac{dm_v}{dt} = \alpha 4\pi R^2 \sqrt{\frac{1}{2\pi \bar{R}_v}} \left[p^*_v \frac{1}{\sqrt{T_{L_i}}} - p_v \frac{1}{\sqrt{T_{g_i}}} \right]$$

where $p^*_v = p_{v_{sat}}(T_{L_i}) \exp\left(-\left(\frac{2\sigma}{R}\right)\left(\frac{v_L}{\bar{R}_v T_{L_i}}\right) \right)$ (5)

$$p_i = \rho_i \bar{R}_i T_g \tag{6}$$

$$p_v = \rho_v \bar{R}_v T_g \tag{7}$$

$$\gamma_1^2 = (T_{L_i} - T_\infty)^2 = \left\{ \frac{d}{dt}\left(\frac{R^3}{3}\rho_v\right) + \frac{\dot{q} R^2}{h_{fg}} \right\} \cdot$$

$$\left\{ \frac{3h_{fg}^2 \alpha_L}{2k_f^2 R^4} \left[\frac{1}{3}\left(R^3 \rho_v(R) - R_o^3 \rho_v(R_o)\right) + \int_o^t \frac{\dot{q} R^2 dt}{h_{fg}} \right] \right\} \tag{8}$$

$$T_{L_i} = T_{g_i}$$

$$\frac{\delta T}{T^2} = \frac{h_{fg}}{4\pi R^2} \frac{dm_v}{dt} + \dot{q} - \frac{dm_v/dt}{4\pi R^2} \left(h_g - \frac{k}{k+1} h_{fg} \right) / L_k \tag{9}$$

The bubble contents temperature gradient calculation (below) requires some explanation. At some time t_o the bubble has an internal temperature profile given by $T_g(r, t_o)$ with an average temperature $T_g(t_o)$. If the contents of the bubble are taken as an open thermodynamic system, then the net rate at which work is being done on the system per unit surface area at time t_o is:

$$\dot{W} = \frac{p_g \dot{R}}{(J)} - \frac{\dot{m}_v}{4\pi R^2} \left\{ \left[h_g(T_{g_i}) + C_{p_v}(\bar{T}_g - T_{g_i}) \right] - \left[u_g(T_{g_i}) + C_{v_v}(\bar{T}_g - T_{g_i}) \right] \right\} + \frac{1}{(J)} \cdot \frac{3m_i}{20\pi R^2} (\dot{R}\ddot{R}) \tag{10}$$

where the first term on the right is the actual work rate, the second and third terms correct for the energy of the vapor mass which leaves the system (condensation), and the last term is the rate of change of the kinetic energy of the bubble contents.

If W from Eq. (10) is assumed to remain relatively constant over a small time interval Δt, then $4\pi R^2 \dot{W} \Delta t$ is the total energy input into the bubble over that interval. Part of this energy goes into increasing the internal energy of the contents, the rest being conducted out of the bubble as heat. To make this division, all of the energy input $\dot{W}\,\Delta t$ first is assumed to go into increasing the internal energy of the contents; the temperature profile $T_g(r, t_o)$ is increased uniformly by an incremental $\Delta T = 4\pi R^2 \dot{W} \Delta t / m_g C_{v_g}$ where $m_g C_{v_g} = m_i C_{v_i} + m_v C_{v_v}$, so that the local temperature at the beginning of the time step is simply $T_g(r, t_o) + \overline{\Delta T}$. The temperature at the interface is assumed constant at $T_{g_i}(t_o)$ over the time interval Δt, and then the problem can be treated as the classical heat conduction problem mentioned previously, solved in Carslaw and Jaeger's classical text[15] The solution for the present case with fixed surface temperature T_{g_i} and initial temperature profile $f(r) = T_g(r, t_o) + \overline{\Delta T}$ is·

$$T_g(r,t) - T_{g_i} = \frac{2}{Rr} \sum_{n=1}^{\infty} \exp\left(\frac{-\alpha_L n^2 \pi^2 \Delta t}{R^2}\right) \sin\left(\frac{n\pi r}{R}\right) \cdot \int_o^R r' f(r') \sin\left(\frac{n\pi r'}{R}\right) dr' \tag{11}$$

After Eq. (11) is evaluated for the new temperature profile (at $t_o + \Delta t$), a new mean temperature can be calculated for the contents of the bubble $\overline{T}_g = \overline{T}_g(t_o + \Delta t)$. The part of the work done which has gone into increasing the internal energy of the gas is then just

$$\Delta u = m_g C_{v_g} \left(\overline{T}_g (t_o + \Delta t) - \overline{T}_g (t_o)\right) \tag{12}$$

and the remainder of the energy has been conducted across the interface, so that

$$\dot{q} = \frac{m_g C_{v_g} \left(\overline{T}_g (t_o + \Delta t) - \overline{\Delta T} - \overline{T}_g (t_o)\right)}{4\pi R^2 \Delta t} \tag{13}$$

In addition to the above equations, we have the following initial and boundary conditions

$$R(0) = R_o, \quad \dot{R}(0) = 0, \quad T(r,0) = T_\infty \text{ for all } r, \quad T_L(\infty, t) = T_\infty, \quad p_v(0) = p_{v_o} = p_{v_{sat}}(T_\infty), \text{ and } p_i(0) = p_{i_o} \tag{16}$$

The system of equations and initial and boundary condition are non-dimensionalized using appropriate combinations of R_o, ρ_L, Δp ($= p_\infty - p_{i_o} - p_{v_o}$), T_∞ and C_{p_L}.

Early calculations in the present study showed that for a cavitation bubble collapsing under one atmosphere overpressure in room temperature water, the interface temperature differential (Eq. (9a)) was $\sim 5\text{-}10^{\circ}F$ in the late stages of collapse. However, this discontinuity does not affect the results significantly because the total temperature difference between the bubble contents and the liquid in the same stages of collapse is very much larger, i.e , thousands of degrees. The irreversible effects were subsequently excluded from the system of equations especially when it was found that they had a highly unstabilizing effect on some solutions; hence, Eq. (9) was used rather than Eq. (9a). A similar unstabilizing effect was produced on some solutions when Eq. (8) was included in the analysis; as discussed in section (3) of the results T_{L_i} was assumed equal to T_∞ throughout many of the cases.

The system of equations (Eqs. (1)-(13)) along with the initial and boundary conditions (Eq. (14) completely describe the collapse. Eqs. (4) and (5) were simultaneously integrated using Hamming's modified predictor-corrector method; Eqs. (6), (7), (9), and (11)-(13) were solved at the same time, with T_{L_i} and W (Eq. (10)) held constant over each time step. The remainder of the calculation for an individual time step consists of evaluating Eq. (8) for T_{L_i}, determining the local pressures and velocities at various points in the liquid from Eqs. (3) and (1), respectively, and

calculating a new value of W from Eq. (10). The whole sequence of calculations is then repeated for subsequent time steps.

III RESULTS AND DISCUSSION

The list of parameters studied, with effects of phase change, spatial temperature variation inside the bubble, and presence of non-condensable gas all included in the analysis, consists of the following:

(1) Proportion of water vapor in the bubble

(2) Evaporation coefficient

(3) Liquid temperature: variable vs. constant

(4) Bubble radius

(5) Thermal conductivity of gas-vapor mixture

(6) Liquid overpressure

(1) Presence of Water Vapor in Bubble

The bubble with only non-condensable gas within was studied previously by Hickling[6] His results can be compared with our own which include the presence of some water vapor within the bubble. Both studies have considered a bubble of 1 mm. radius with an internal nitrogen pressure of 0.075 atmospheres, an external overpressure ($=p_{\infty} - p_{i_o} - p_{v_o}$) of 2.925 atmospheres, and a uniform initial temperature of 68°F. Our calculation includes the effect of the vapor, while Hickling's does not.

Fig. 2 shows a direct comparison of the temperature profiles within the bubble in the two cases at various present to initial radius ratios. The x's show the actual data points resulting from the water vapor calculation, while the solid line is a smoothed approximation. There is good agreement between the two calculations; one expects, as Hickling has pointed out, somewhat lower temperatures with the water vapor present merely because those molecules are triatomic. The adiabatic state relation, $Tv^{\gamma-1} = \text{Constant}$, which gives an upper limit for the internal temperature rise during collapse, will yield larger values of T for diatomic gases ($\gamma = 1.4$) than for triatomic gases ($\gamma = 1.33$) for a given volume

reduction. On the other hand, the thermal diffusivity is reduced by the addition of water vapor to the nitrogen gas, tending to produce higher temperatures as the bubble collapses more nearly adiabatically. The polytropic exponent increases only slightly from about 1.30 near the beginning of collapse to about 1.34 near the start of rebound. The adiabatic value for a bubble whose initial contents are 85% nitrogen gas and 15% water vapor is 1.38.

(2) Evaporation Coefficient

The value chosen for the evaporation coefficient α in Eq. (5) can be expected to have a most important effect. α is the correction factor known as the absorption or evaporation coefficient, and represents the ratio of experimentally observed evaporation rates to those predicted by the right-hand side of Eq. (5) with α equal to one. α has experimentally been shown to take on a wide range of values between 0 and 1. Theofanous, Biasi, and Isbin[16] give a good summary of recent experimental research on this important parameter, and, in a subsequent paper, Theofanous et al[8] suggest that 5×10^{-2} may be an appropriate value for α for water. It depends on various relatively unpredictable physical parameters such as interface contamination, etc. Three values have been assumed for α in this portion of the analysis: 0.01, 0.1 and 1.0.

Figs. 3-6 show some of the results from this calculation. The bubble in this case contained air at initial partial pressure of 10^{-3} atmospheres and water vapor (saturated at 77°F) at pressure of 0.0276 atmospheres (i.e., initial vapor mass fraction of total = 95%). The external pressure far from the bubble is assumed constant at one atmosphere.

Fig. 3 shows the effect of α upon the portion of vapor not condensing. For the smallest value of α (0.01), about 50% of the vapor would remain at the conclusion of the calculation (at start of rebound), while for $\alpha > 0.1$ $< 3\%$ of the original vapor would remain at radius ratios (R/R_o) of 0.01. For the larger α(s), the wall velocity continues to increase monotonically throughout the calculation, with virtually all of the vapor condensing before

high collapse velocities develop. Thus in this case the collapse is essentially that of a bubble containing only the non-condensable gas. For $\alpha = 0.01$, however, the vapor has a definite retarding effect; the bubble wall reaches a peak dimensionless velocity of 30.6 at $R/R_o = 0.057$ and rebounds shortly thereafter from a minimum radius of $R/R_o = 0.041$.

Fig. 4 confirms the above. There is only a very slight difference (not distinguishable in the figure) between the radius history of the $\alpha = 1.0$ case and the radius history of an identical empty Rayleigh bubble down to $R/R_o = 0.03$. Thus, only a single dotted curve is shown for both cases. For $\alpha = 0.01$ significant retardation of the collapse begins when R/R_o is still greater then 0.5, although this does not show in Fig. 4 until later.

Fig. 5 shows the history of the total (vapor plus non-condensable gas) pressure inside the bubble. The conclusion from these curves is that the lower the contents pressure over the early part of the collapse, the higher will be the peak pressure inside the bubble at the conclusion of collapse, and hence presumably the greater the damage capability of the cavitation bubble upon rebound. Therefore, the more rapidly the water vapor condenses (i.e., the larger the value of α), the more likely it is that damage will occur. If α is actually very low, then little of the vapor will condense, and rebound will commence with substantially lower pressures inside the bubble. Moreover, the further that collapse proceeds before the internal gas pressure begins to retard the inward motion of the wall, the greater will be the buildup of inertia in the liquid, and hence the greater the overshoot beyond the bubble equilibrium radius.

This effect of the evaporation coefficient seems to establish a paradox if shock waves from the rebounding bubble are in fact a primary damage cause. If a bubble initially contains mostly saturated water vapor with only a little non-condensable gas, then the evaporation coefficient α must be very large ($\rightarrow 1.0$) to insure high enough peak pressures to subsequently cause damage. Conversely, it appears likely that it is actually much less than 1.0 (as indicated in ref. 8) in low gas content bubbles, since otherwise sonoluminescence would be much more commonly observed in cavitation bubbles collapsing in water.

Fig. 6 (average gas temperature as function of bubble radius) shows that the more rapidly the vapor condenses, the slower will be the temperature buildup inside the bubble. The primary cause of this variation is most likely the larger thermal diffusivity which arises from the lower contents density in the larger α cases. The slower temperature buildup produces both lower pressures and eventually lower peak temperatures within the bubble.

(3) Variable vs. Constant Liquid Temperature

For bubbles only slightly subcooled, it is obvious that the variation in liquid temperature near the interface can be very critical. For highly subcooled bubbles (characteristic of many cavitation cases), the effect of the liquid temperature increase during collapse is not so important, as perhaps best shown analytically by Florschuetz and Chao[7]. Various experiments have also demonstrated this with respect to actual cavitation damage production, including work by one of the present authors[17]. Figs. 7 and 8 show some of the effects of allowing the liquid temperature to vary in the calculation by comparing the resulting collapse conditions with those under a constant liquid temperature assumption, i.e., liquid with infinite thermal diffusivity. The initial bubble conditions are identical to those in the previous section with α equal to 0.1.

Fig. 7 shows that the internal pressure of the gas-vapor mixture is only slightly less throughout the collapse if constant liquid temperature is assumed than if the actual variable temperature is used. The difference can be attributed to the higher rate of evaporation from the liquid surface when the temperature increases (hence a lower net rate of condensation (see Eq. (7)), and to the higher temperature of the contents in the latter case. In Fig. 8, the liquid temperature at the interface can be seen not to change by more than 10% until R/R_o is less than 0.3. The increase in T_{L_i} for smaller radii causes a corresponding divergence in condensation rates, as explained above. Because of the only slight differences in all the curves of Figs. 7 and 8, and because more than 85% of the initial vapor will have condensed when R/R_o 0.3 (Ref. Fig. 3 for α 0.1), we conclude that the variation in liquid temperature produced by release of the latent condensation

heat and by heat conduction out of the bubble will have a negligible effect on the collapse of a highly subcooled cavitation bubble of the type here studied.

(4) Bubble Radius

For smaller maximum (initial) bubble radii, one expects the collapse process to become more and more isothermal, at least during the early stages, because the resistance to heat flow from the interior of the bubble out to the liquid is reduced, i.e., the ratio of surface area to volume for small bubbles is more favorable. The initial conditions other than maximum radius are the same for this calculation as in the previous section. Calculation of the polytropic exponent γ (assuming p/ρ^{γ} = Constant over short segments of the collapse) at various points during the collapse, shows that the collapse becomes more and more adiabatic as it proceeds, approaching as an upper limit the adiabatic exponent (1.33 for the initial mixture of air and water). γ takes on values between 1.00 and 1.20 during the early stages of collapse for the smallest bubble calculated ($R_o = 0.5 \times 10^{-3}$ in), between 1.10 and 1.20 for a medium bubble ($R_o = 5 \times 10^{-3}$ in), and between 1.24 and 1.30 for the largest bubble calculated ($R_o = 50 \times 10^{-3}$ in). By the time R/R_o reaches 0.05 in the first case, γ is about 1.30.

The net effect of the lower contents temperature in smaller bubbles on the damage capability of smaller bubbles appears to be negligible. According to Fig. 10, the gas-vapor total pressure does not significantly differ between the three initial size cases throughout their collapse histories.

(5) Thermal Conductivity of Gas-Vapor Mixture

An additional parameter of interest is the thermal conductivity of the bubble contents. The same initial bubble conditions were used for this calculation as in the previous three sections ($R_o = 50 \times 10^{-3}$ in., $p_{i_o} = 10^{-3}$ atm, $p_{v_o} = p_{v_{sat}}$ (77°F), $T_{\infty} = 77^{\circ}$F, $\alpha = 0.1$), but the actual thermal diffusivities of the contents was replaced in two different cases by the extrema values, zero and infinity. The first corresponds to the adiabatic case giving uniform but not constant temperature in the bubble, and the second to a constant temperature of bubble contents.

Figs. 11 and 12 show the effect of this range of thermal diffusivities of the bubble contents on the pressure history of the bubble, on the average temperature of the contents, and on the rate of vapor condensation. The pressure record shows no significant difference between either of the extreme values and the true value of the thermal diffusivity; in fact, the adiabatic (zero thermal diffusivity) collapse pressure history can be represented by the same curve as that for the true value of thermal diffusivity.

The essentially adiabatic nature of the typical cavitation bubble collapse is further confirmed in Fig. 12. The average temperature of the contents is greater than 90% of the adiabatic temperature at the corresponding radii ratio throughout the collapse. The rates of condensation in the three cases are quite similar, about 80% of the vapor mass having condensed by the time R/R_o reaches 0.3 in the infinite diffusivity case; more than 85% in the other two cases.

(6) Liquid Overpressure

Experiments in this laboratory and elsewhere[18, e.g.] have shown that the greater the difference between the initial bubble internal pressure and the system pressure far from the bubble, the greater will be the cavitation damage rate. This pressure effect can be explained with the aid of Figs. 13 and 14, which show the internal pressure histories of the "standard" bubble described in the previous sections, collapsing under 1, 2 and 4 atm. overpressure. According to Fig. 13, the higher the overpressure, the lower will be the ratio of internal gas pressure to initial pressure differential at a given radius ratio R/R_o. The lower this ratio is in the early stages of collapse, the smaller will be the eventual minimum radius and the higher the eventual pressure ratio. However, according to Fig. 14, the actual internal pressure increases with system overpressure for a given R/R_o. The result is that the greatest initial overpressure produces the smallest miminum radius and the largest peak internal pressure, and thus can produce the most intensely damaging shock waves (or microjet velocities) in agreement with the experiments[18, etc

In addition to the above parameters, the results of the analysis include pressure distributions in the liquid at various points during the collapse. In Fig. 15 one such set of profiles are shown, for a bubble with the same initial conditions employed in sections (2) - (6) above. The profiles are quite similar to those reported by Ivany and Hammitt[4] in their analysis which includes compressibility effects but does not include phase change or thermodynamic effects. Substantial pressures ($>10^4$ atm.) arise in the liquid at small radii during collapse. Although high enough pressures during collapse to explain observed damage at distances greater than the bubble initial radius are not obtained, a similar calculation by Hickling and Plesset[3] shows sufficiently high pressures in a shock wave produced upon the rebounding of such bubbles.

CONCLUSIONS

The effects of the various thermodynamic parameters and of phase change are summarized in Table I. The results given are, in general, for a typical highly subcooled cavitation bubble (e.g., $R_o = 50 \times 10^{-3}$ in., $p_{i_o} = 10^{-3}$ atm., $p_{v_o} = 0.406$ psi $= p_{sat}(77^oF)$, $T_o = T_\infty = 77^oF$), $p_\infty = 1$ atm. The effects on damage capability (3rd column of Table I) are based on the hypothesis that damage is caused by a shock wave produced as the bubble begins to rebound from its minimum size. The peak pressure obtained internally and the minimum radius are thus critical factors in establishing the strength of such shock waves. Presumably, at least the directions of variations would be the same if microjet impact is the damage mechanism. Actually, in most cases, it is probably due to a combination of both effects.

As can be seen from the table, the presence of water vapor coupled with the value of the evaporation coefficient and the pressure difference initially between the liquid far from the bubble and its contents are the most significant variables in the present study. As was pointed out in the previous discussion, if the evaporation coefficient α is very large ($\rightarrow 1.0$) the effect of the vapor on the collapse will be relatively small since it will

condense very rapidly, essentially being "blotted-up" by the in-moving wall. For α of the order of 0.01, the most likely magnitude for water[8]* the vapor will have a significantly retarding effect on the collapse.

The thermal diffusivity of the bubble contents has a slightly less important, but still significant effect on the collapse. It appears, however, that cavitation bubble collapses may be assumed adiabatic throughout without disturbing the results very greatly.

The other factors investigated, such as initial bubble radius and the variation of liquid temperature, have been shown to have little effect on the collapse velocity or pressure at a given radius ratio for highly subcooled bubbles. The effect of any non-equilibrium temperature discontinuity at the vapor-liquid interface is also negligible. The calculations indicate further that the vapor will be far from saturation conditions in the later stages of collapse, the bulk of it having condensed.

The present authors and others have shown in recent papers[1, 19, e.g.] that cavitation bubbles will collapse asymmetrically under a variety of real flow conditions. The collapse under such conditions produces liquid jets of sufficiently high velocity to cause impact damage and does so with relatively small volume changes ($R/R_o > 0.25$). The effects discussed in the present paper will probably be of only second order when compared to the asymmetric effects which arise in real flow conditions (e.g., steep pressure gradients, proximity to a solid wall.)

No good experimental values for this coefficient for various fluids and conditions yet exist.

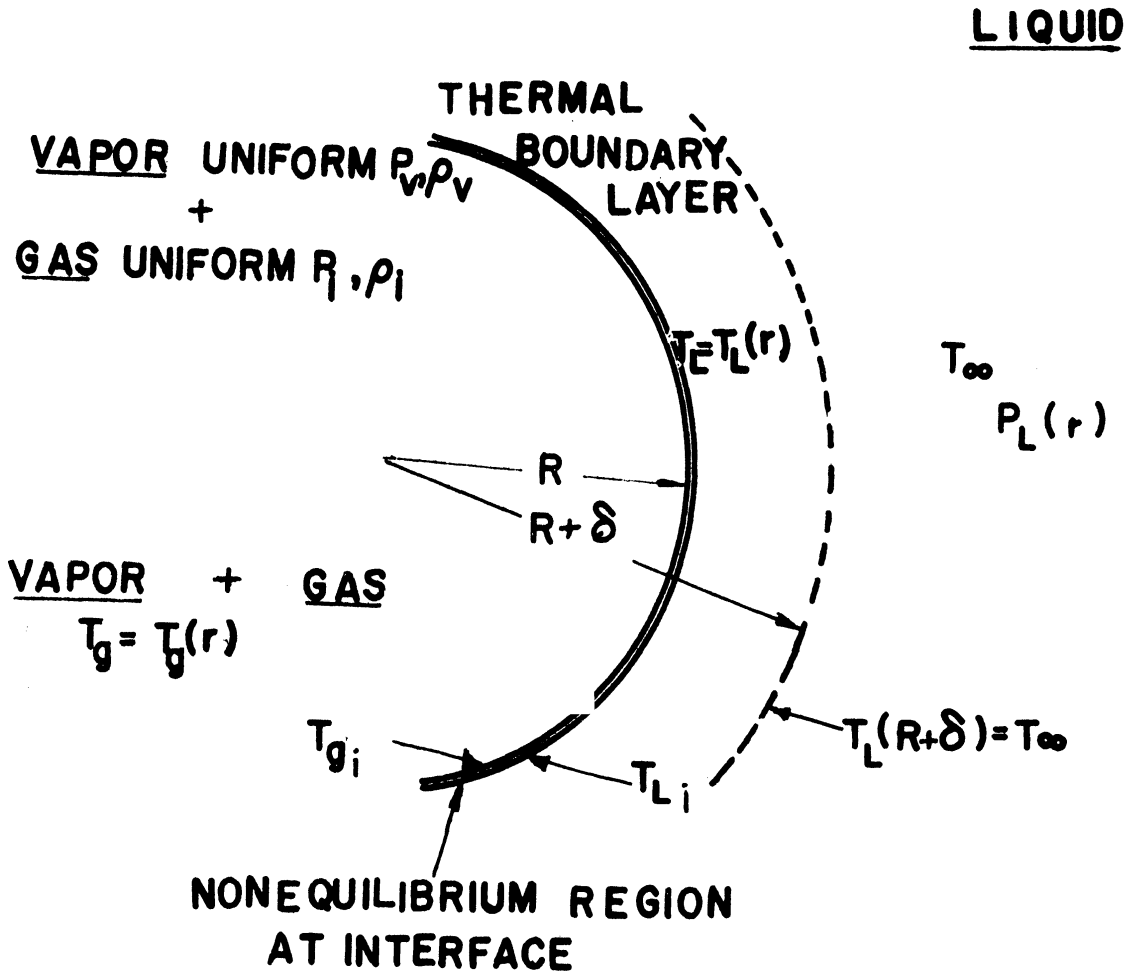

Fig. 1(a). Location of Variables for Thermodynamic Effects Study

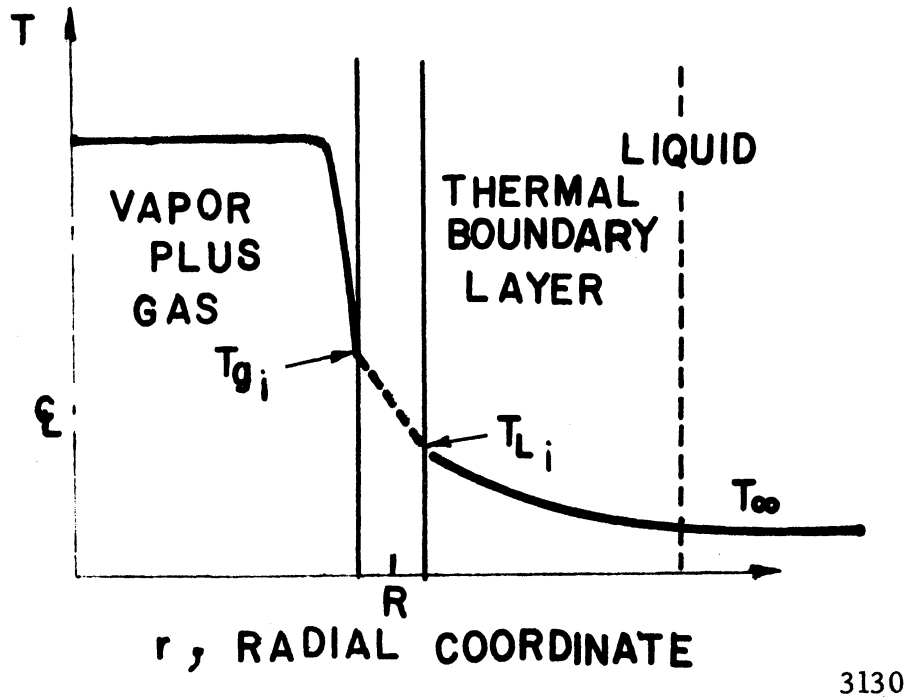

Fig. 1(b). Sample Temperature Profile During Collapse

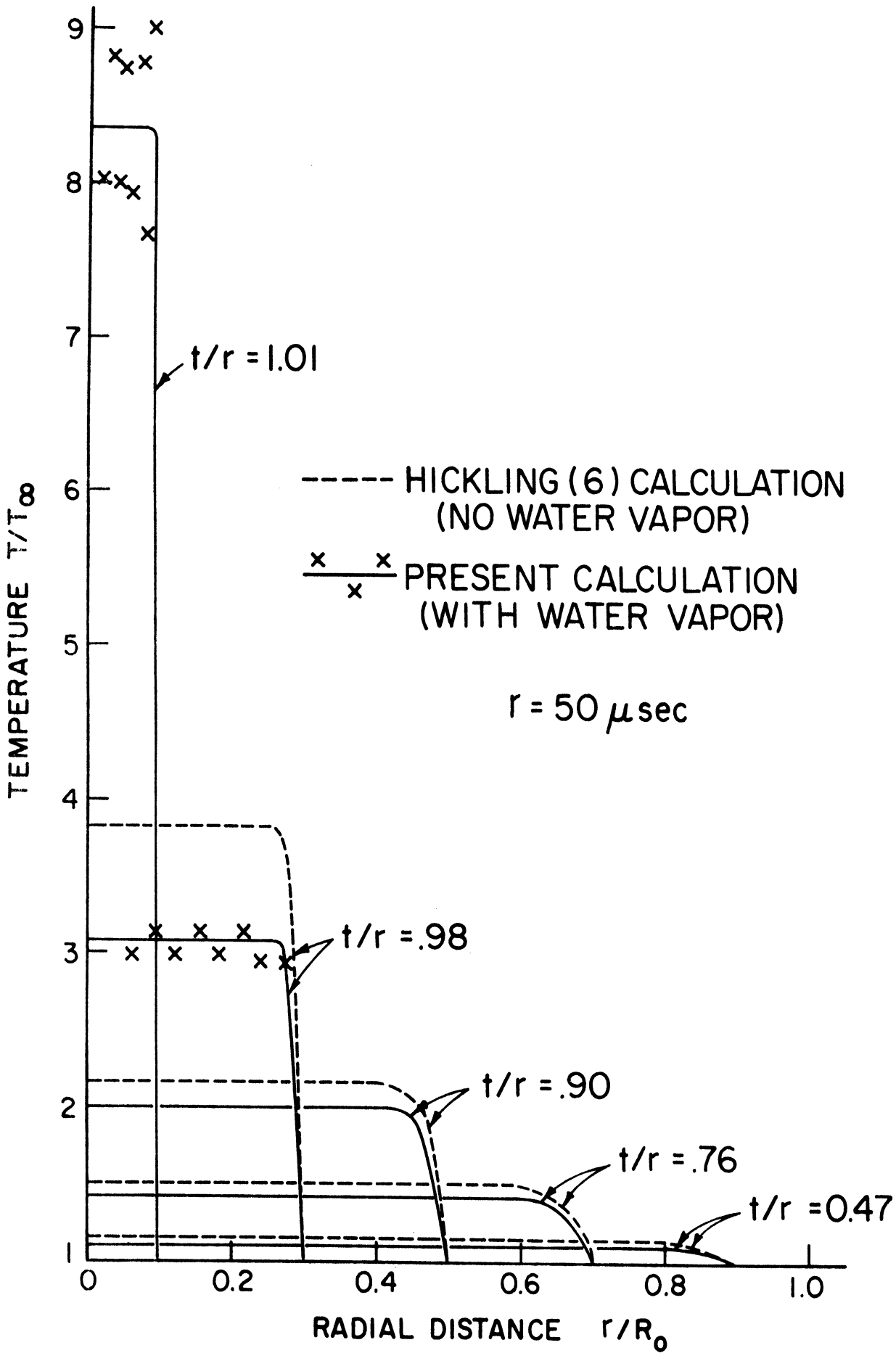

Fig. 2. Internal Temperature Distributions at Different Radii for Bubbles Containing Nitrogen Gas with and without Water Vapor; α 0.1, p_{i_o} = 0.075 atm., p_{v_o} = 0.0277 atm., Δp = 2 925 atm. R_o 0.1 cm., T_o = 528° R.

3131

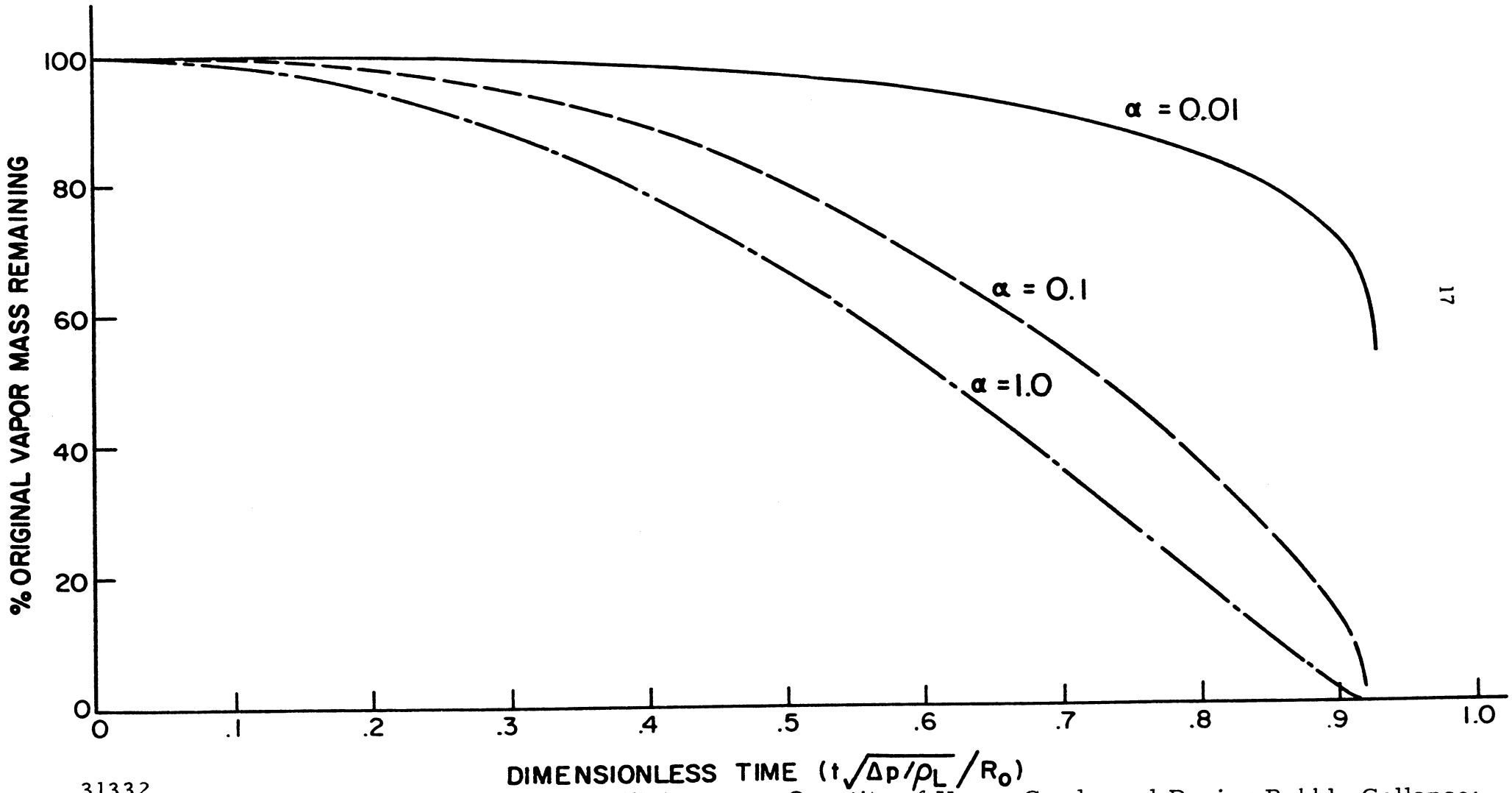

31332 Fig. 3. Effect of Evaporation Coefficient α on Quantity of Vapor Condensed During Bubble Collapse; "Standard" Bubble: $R_o = 50 \times 10^{-3}$ in., $T_o = 537$ R, $p_{i_o} = 10^{-3}$ atm., $p_{v_o} = 0.0277$ atm., $p_\infty = 1$ atm.

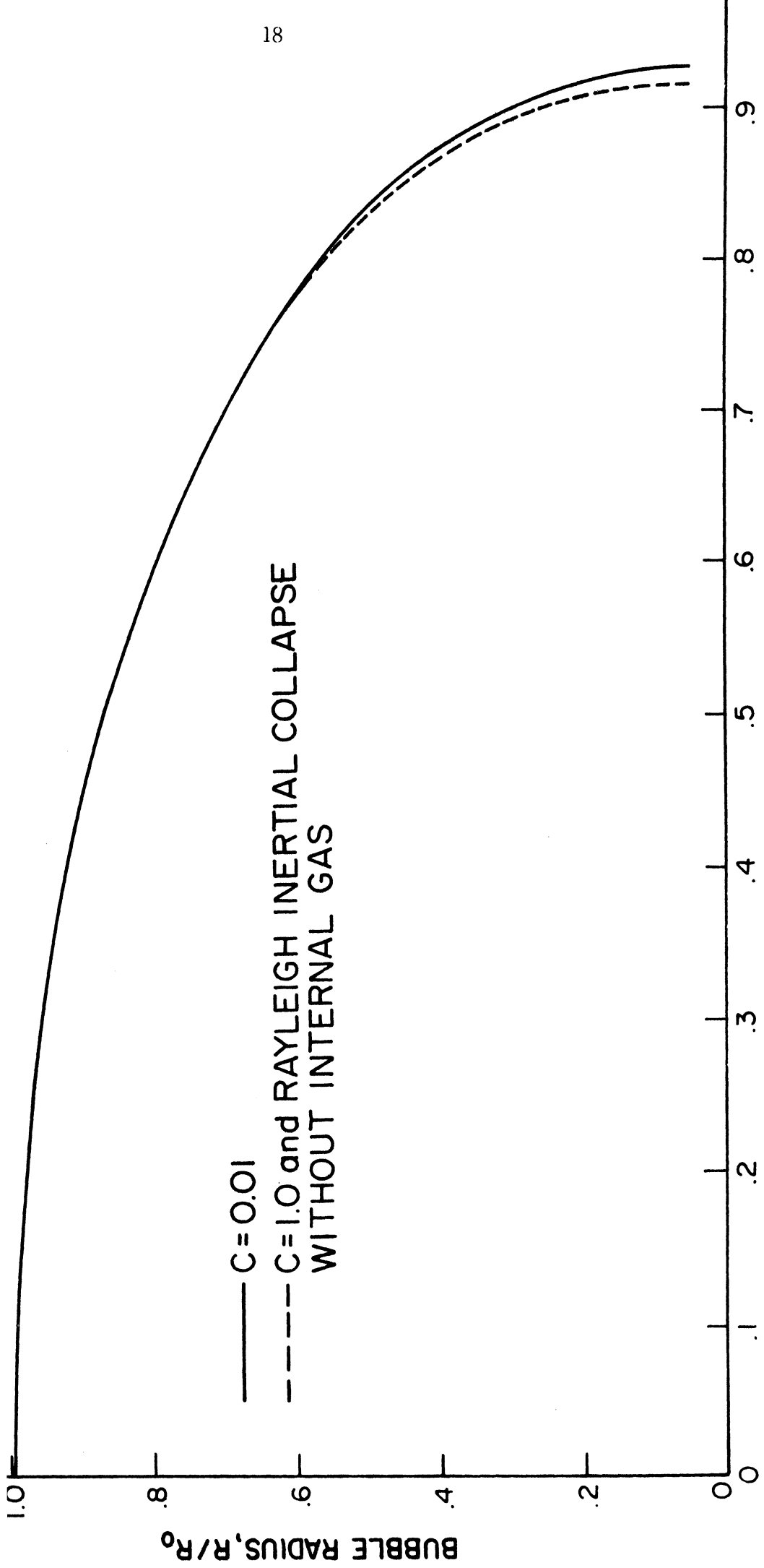

Fig. 4. Effect of Evaporation Coefficient α on Bubble Radius Change with Time for "Standard" Bubble (see Fig. 3)

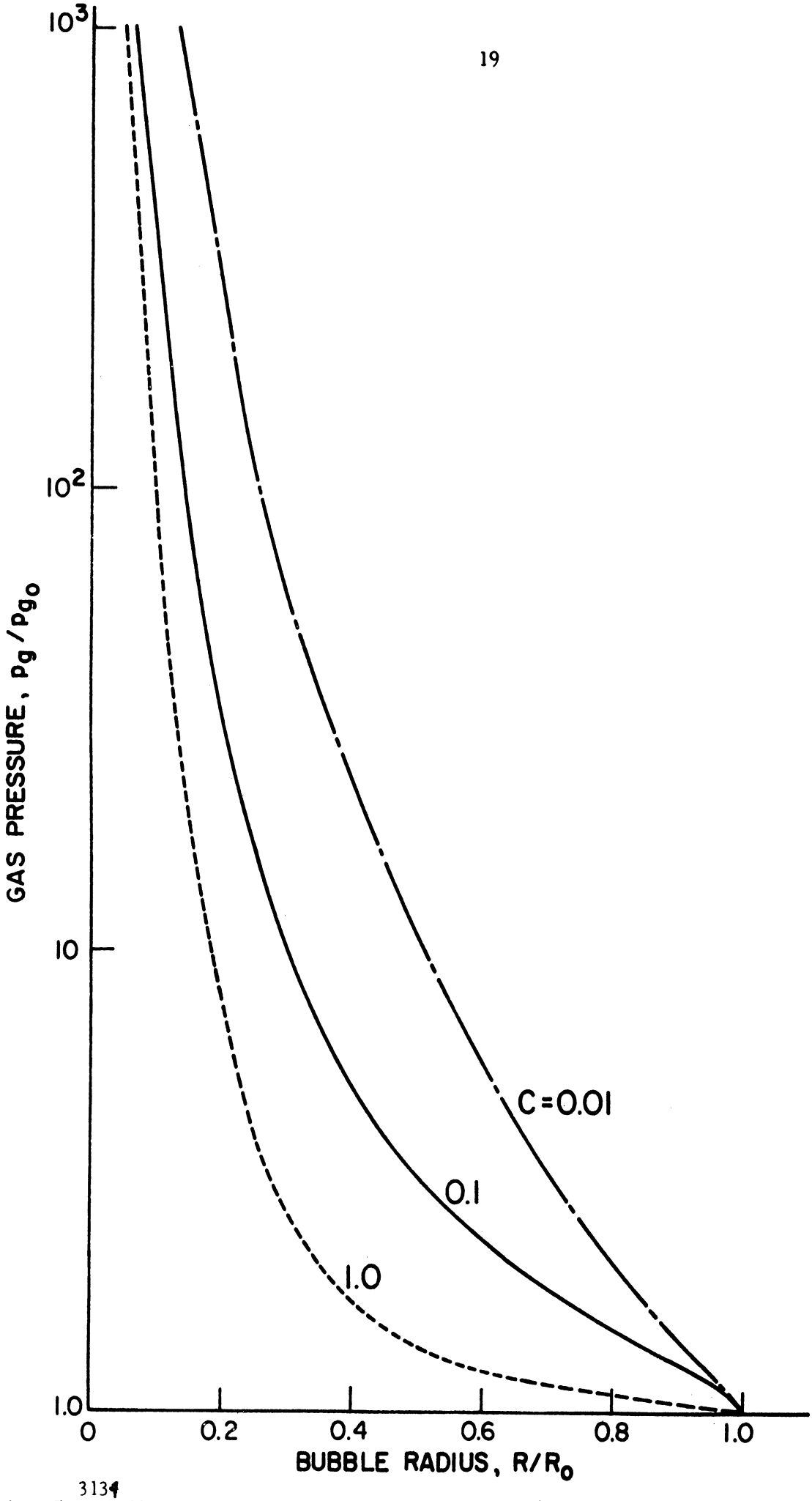

3134

Fig. 5. Effect of Evaporation Coefficient α on Internal (Gas + Vapor) Pressure Change with Radius for "Standard" Bubble (See Fig. 3)

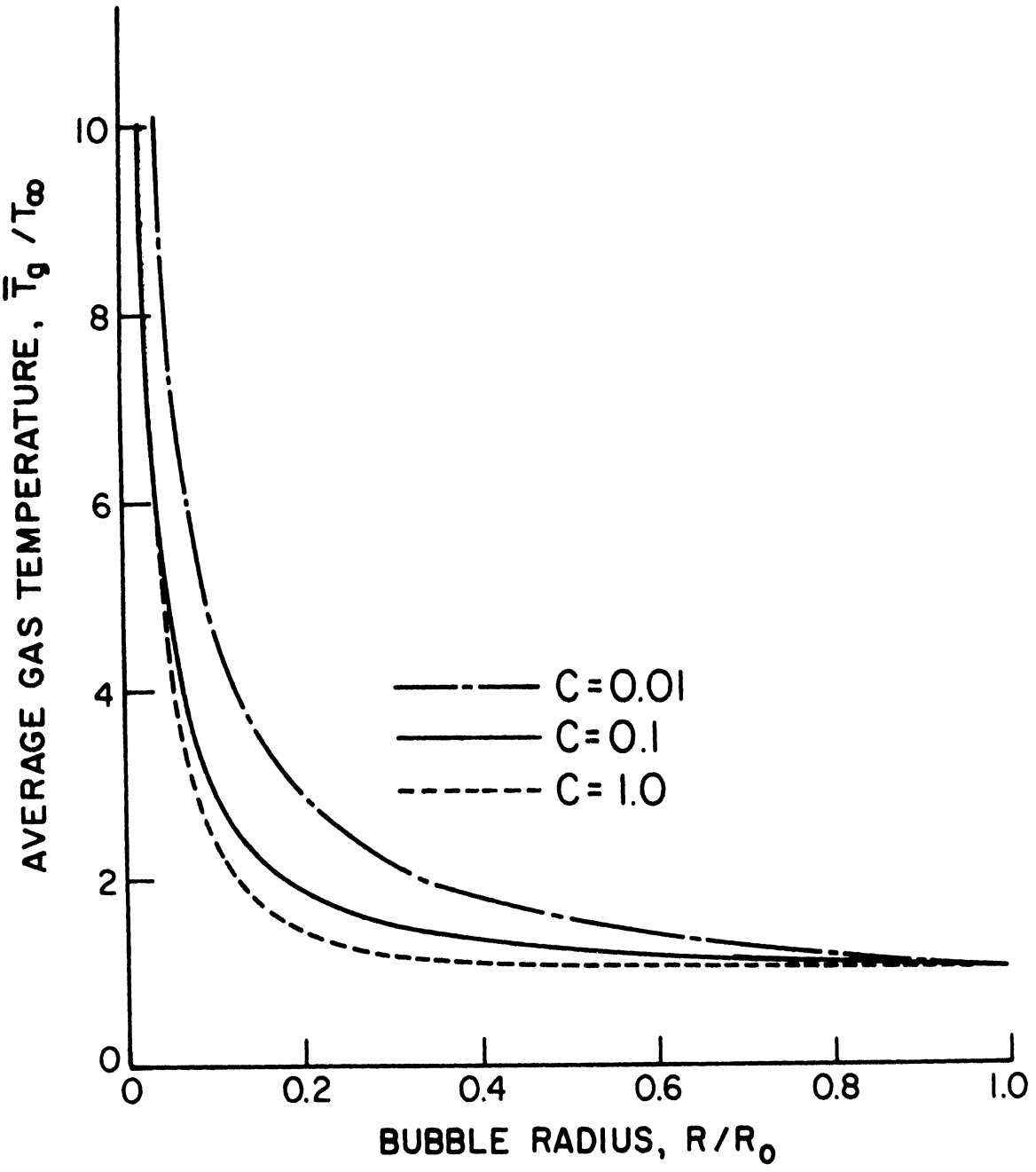

Fig. 6. Effect of Evaporation Coefficient α on Average Internal Temperature Change with Radius for "Standard" Bubble (see Fig. 3).

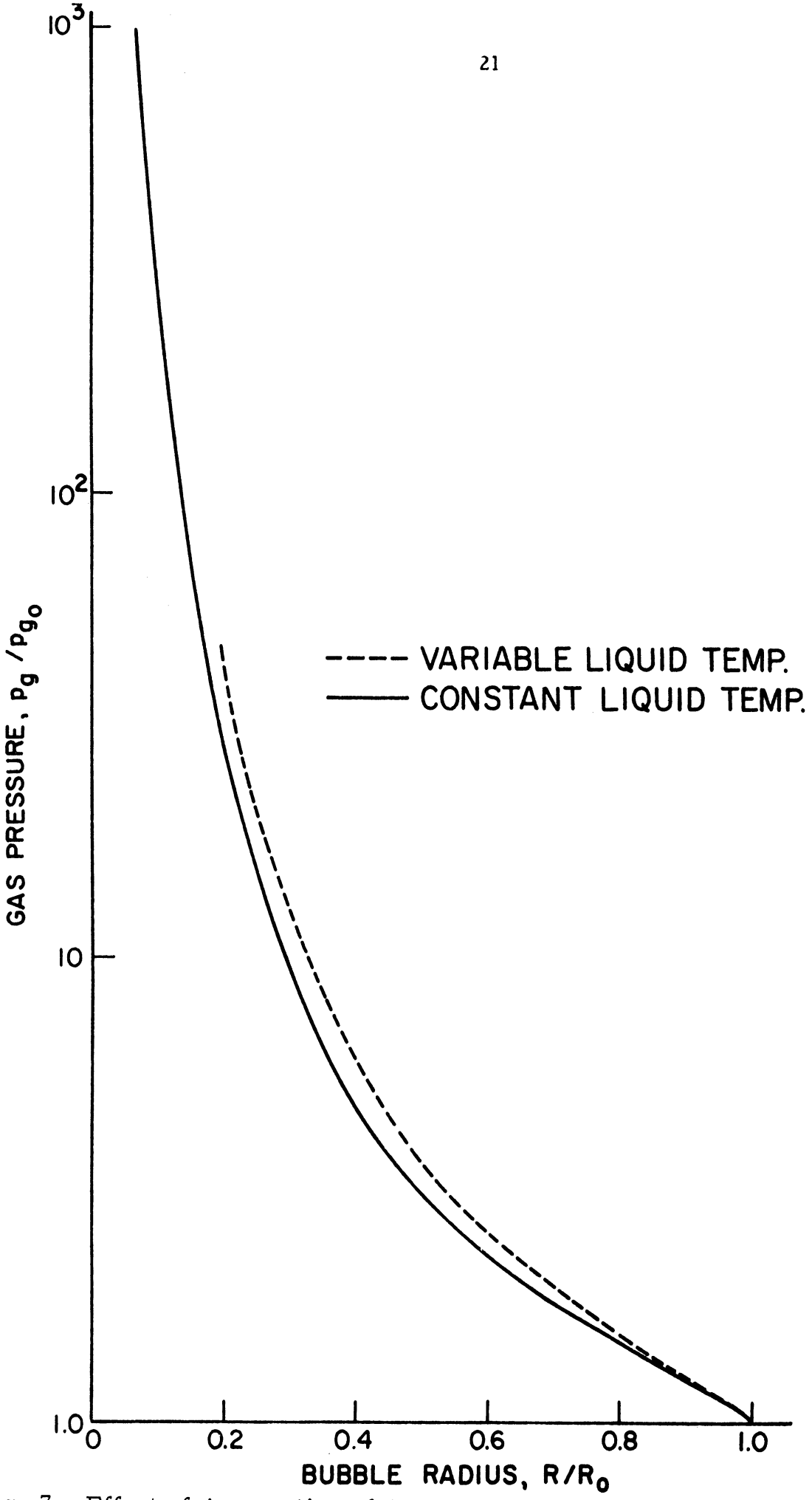

3136

Fig. 7 Effect of Assumption of Constant Temperature in Liquid on Internal (Gas + Vapor) Pressure Change with Radius for "Standard" Bubble (see Fig. 3), $\alpha = 0.1$

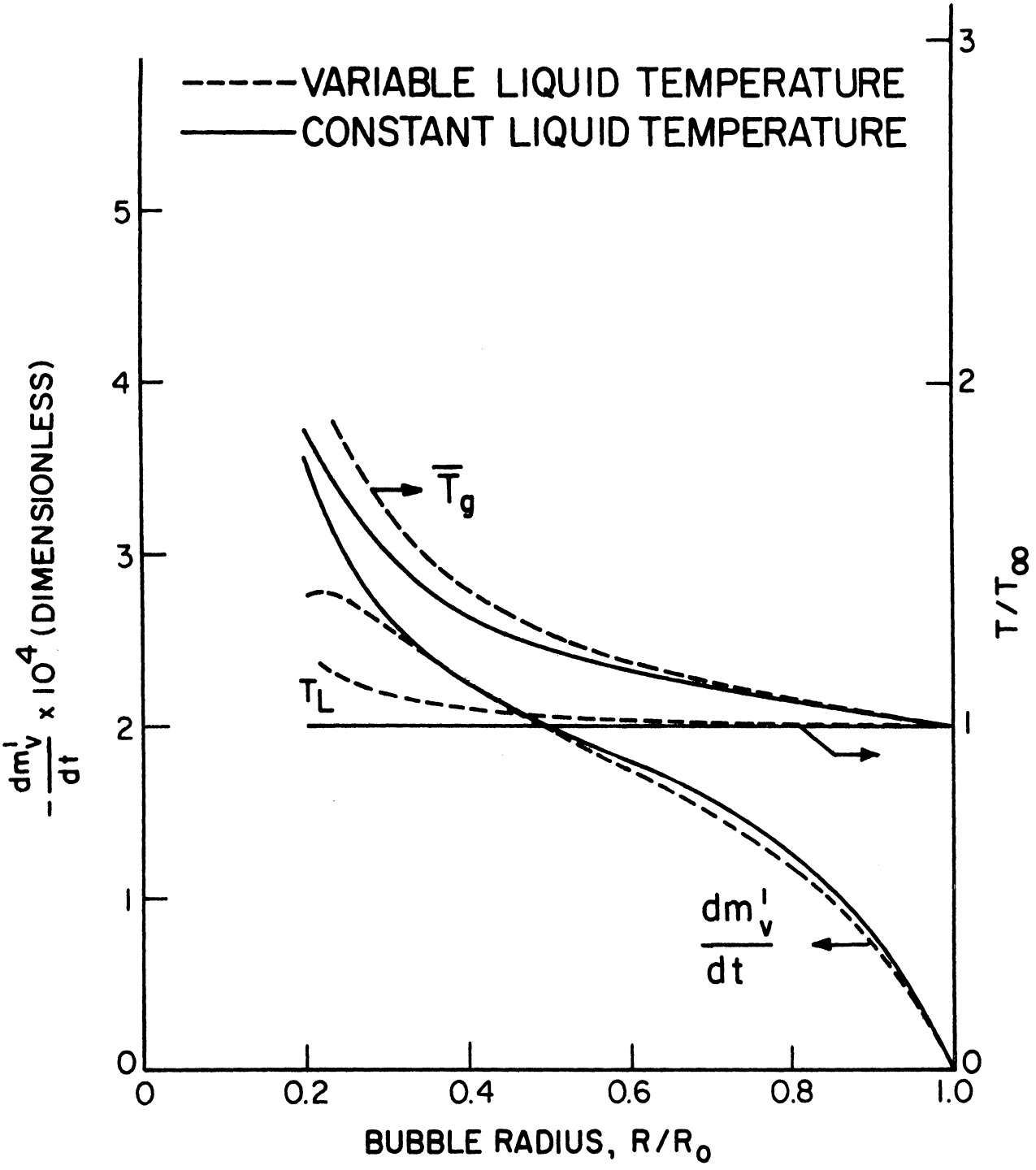

3137

Fig. 8. Effect of Assumption of Constant Temperature in Liquid on Condensation Rate, Average Internal Temperature, and Liquid Temperature at Interface as Function of Radius for "Standard" Bubble (see Fig. 3), $\alpha = 0.1$.

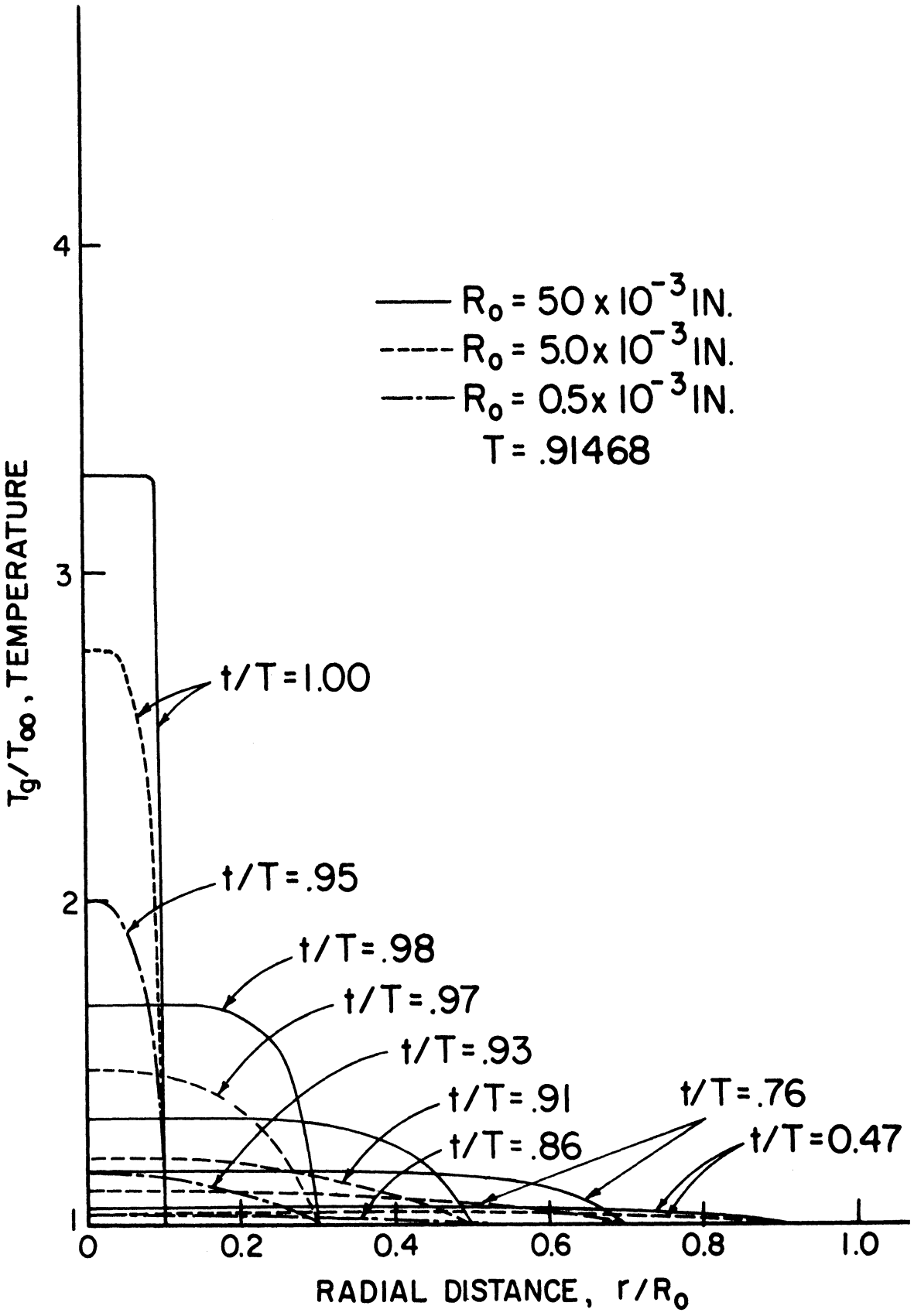

3138

Fig. 9. Internal Temperature Distributions at Different Stages of Collapse for "Standard" Bubbles (see Fig. 3) with Different Initial Radii, $\alpha = 0.1$.

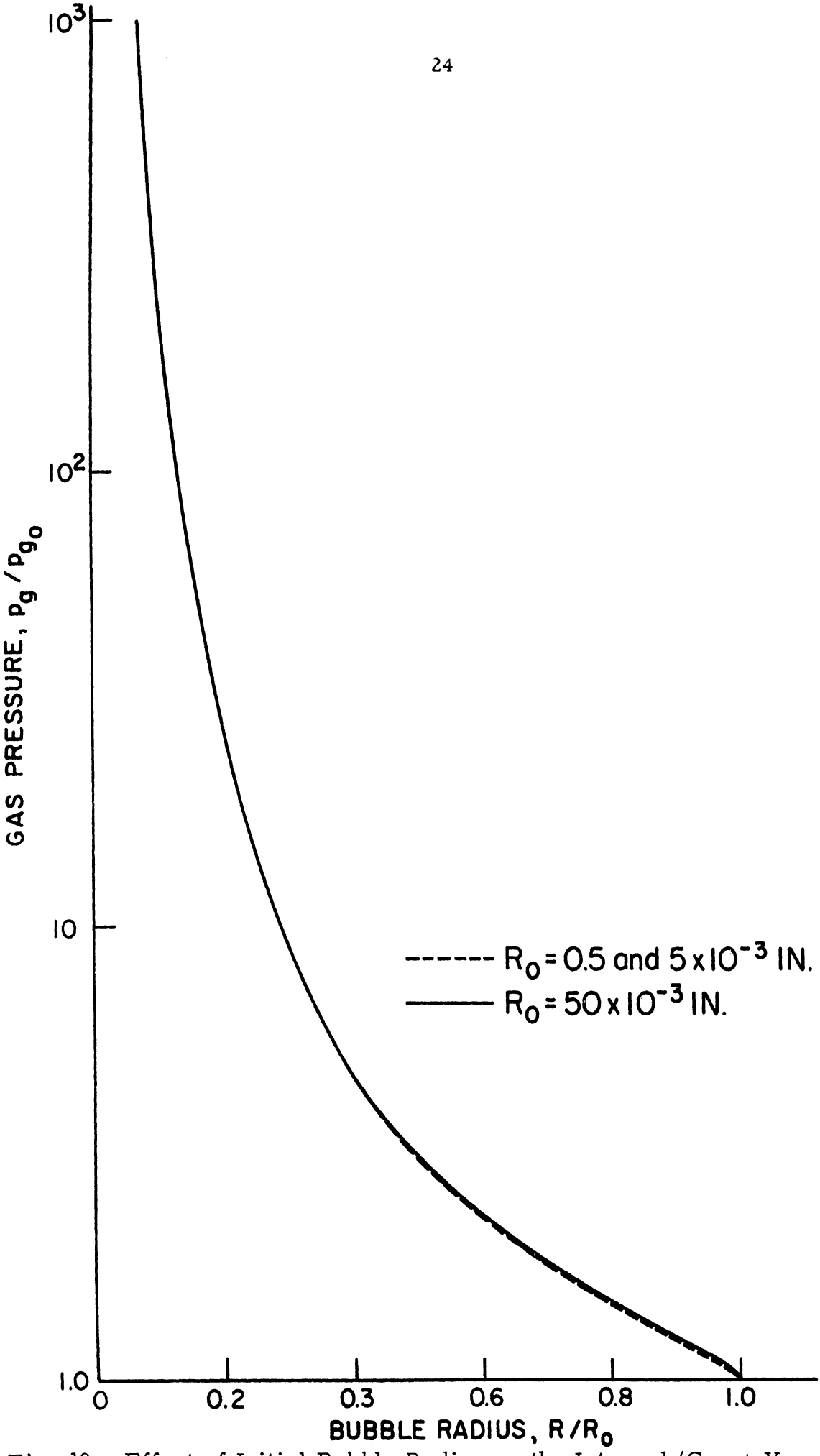

3139 Fig. 10. Effect of Initial Bubble Radius on the Internal (Gas + Vapor) Pressure History During Collapse of Otherwise "Standard" Bubbles (see Fig. 3), $\alpha = 0.1$

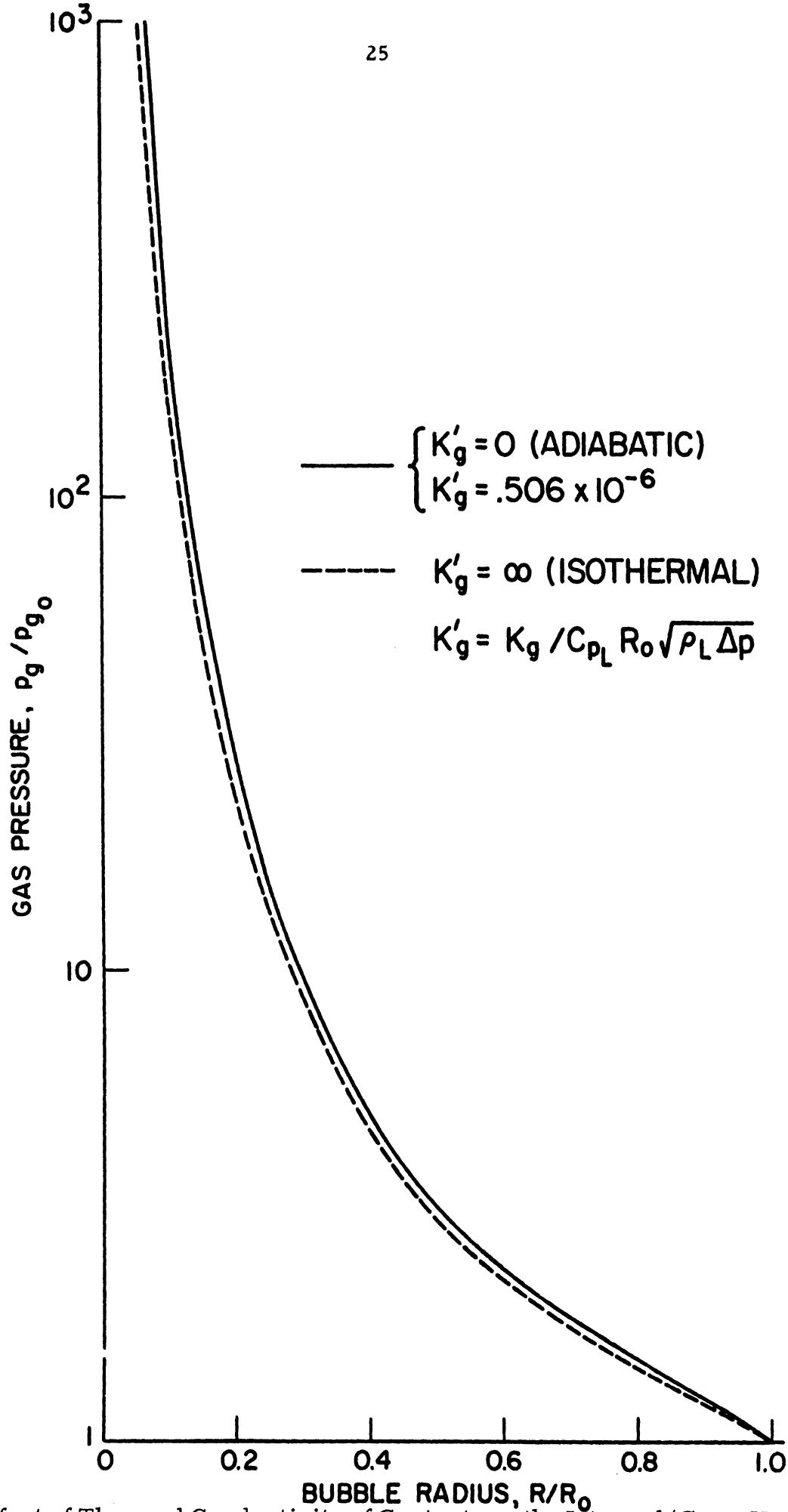

3140 Fig. 11. Effect of Thermal Conductivity of Contents on the Internal (Gas + Vapor) Pressure History During Collapse of "Standard" Bubble (see Fig. 3), $\alpha = 0.1$

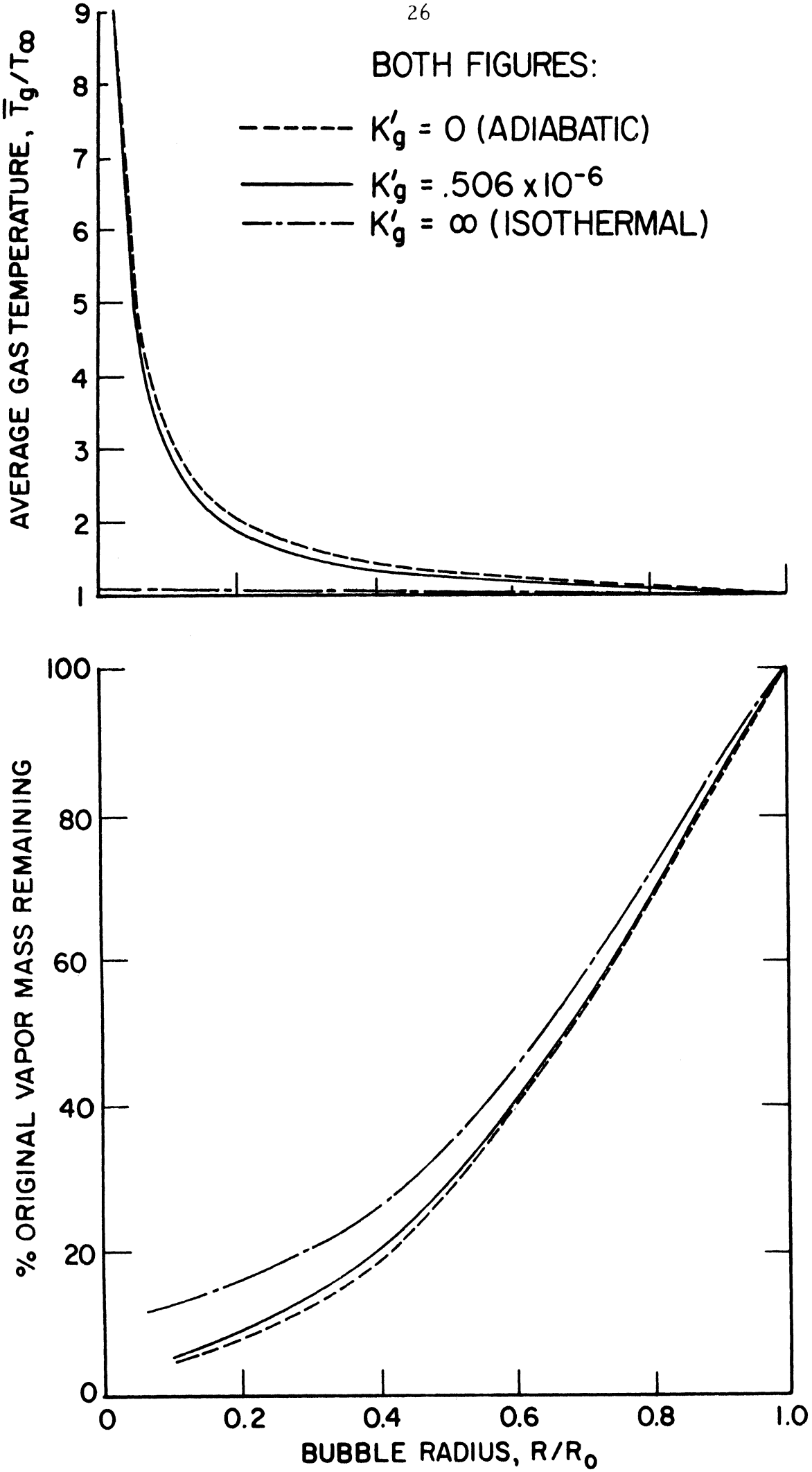

Fig. 12. Effect of Thermal Conductivity of Contents on the Average Internal Temperature on Vapor Condensation Rate as Function of Radius for "Standard" Bubble (see Fig. 3), α =

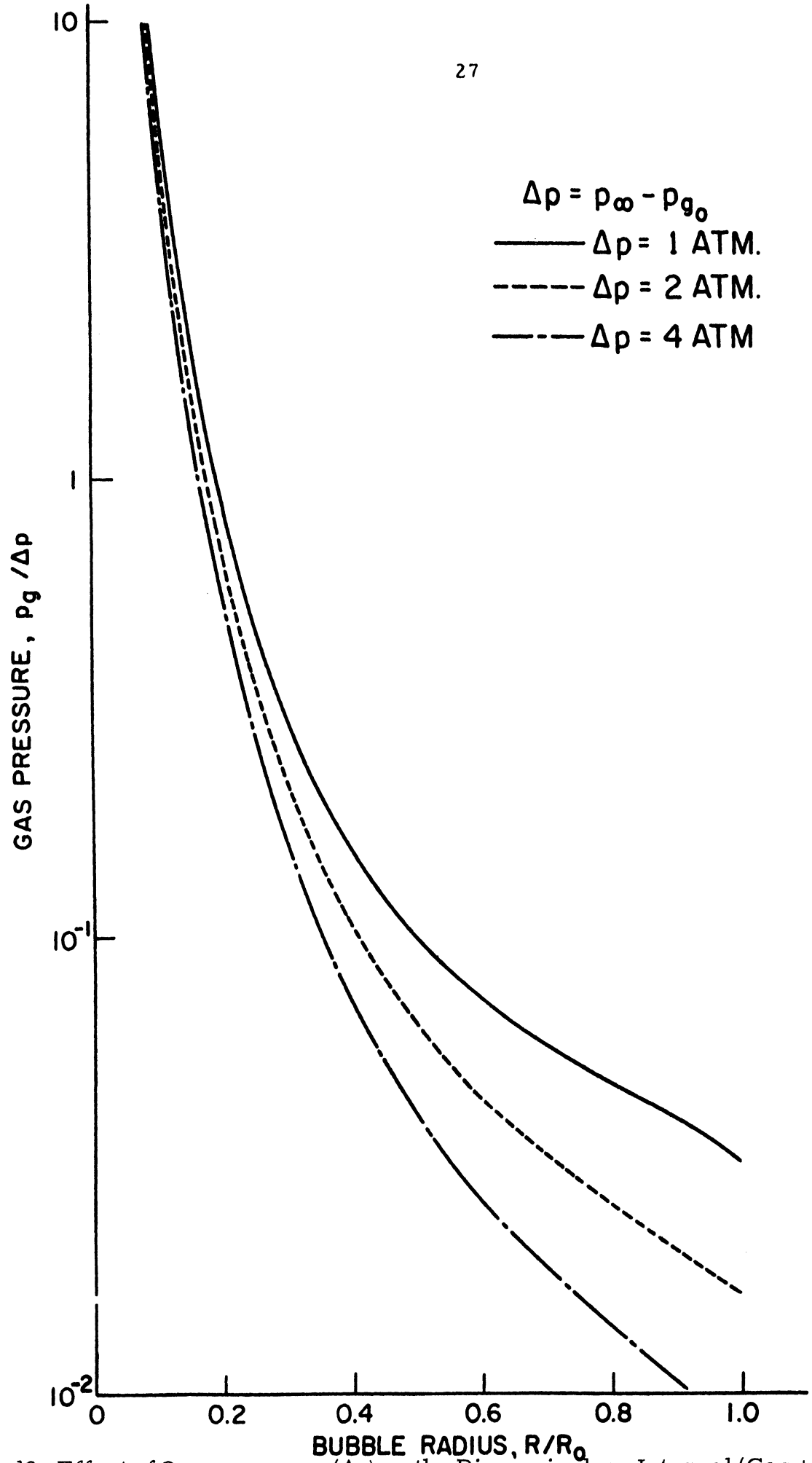

Fig. 13. Effect of Overpressure (Δp) on the Dimensionless Internal (Gas + Vapor) Pressure History of Collapsing Bubbles, $R_o = 50 \times 10^{-3}$ in., $T_o = 537^o$R, $p_{i_o} = 10^{-3}$ atm., $p_{o_v} = 0.0277$ atm. $\alpha = 0.1$

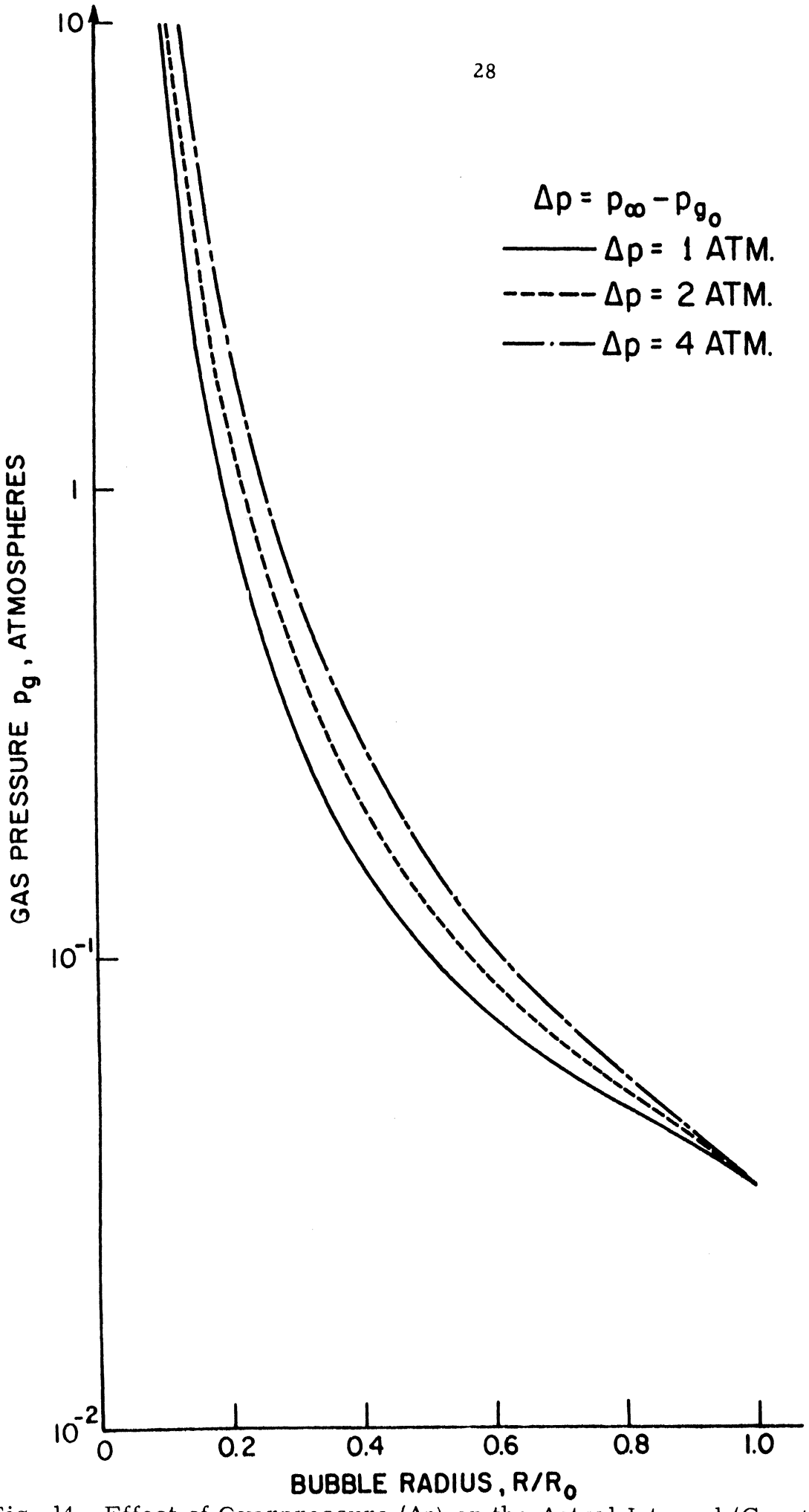

3143

Fig. 14. Effect of Overpressure (Δp) on the Actual Internal (Gas + Vapor) Pressure History of Collapsing Bubbles; Conditions same as for Fig. 3

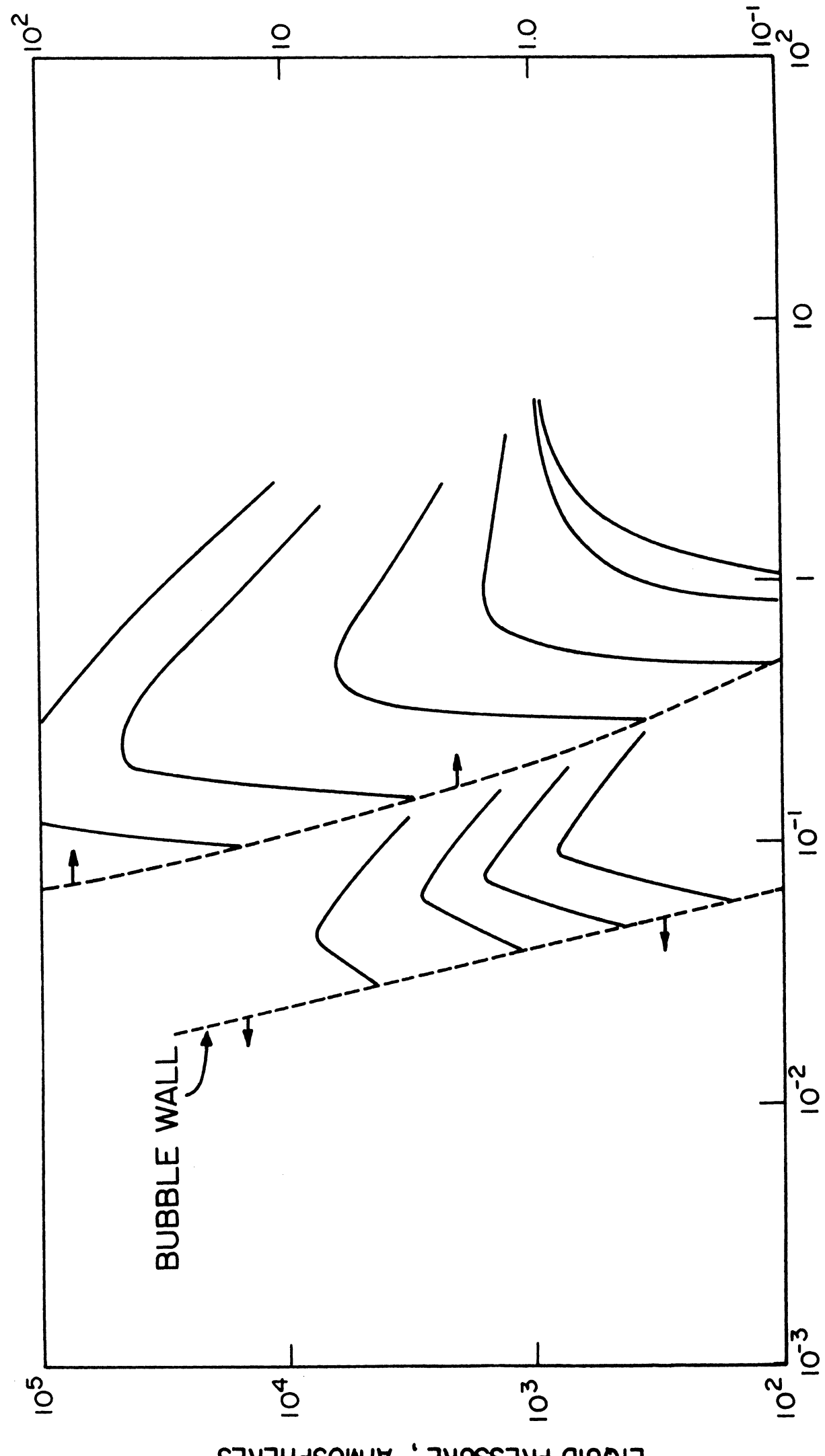

Fig. 15. Pressure Profiles in Liquid at Different Stages of Collapse for "Standard" Bubble (see Fig. 3), $\alpha = 0.1$

TABLE I

EFFECTS OF PARAMETERS ON CAVITATION BUBBLE COLLAPSE

Parameter	Effect Due to Increased Value of Parameter	Significant Effect on Damage Capability
Presence of Water Vapor	Lower Temperatures of Contents	Depends on Actual Value of Evaporation Coefficient
Evaporation Coefficient	Faster Condensation, Higher Peak Pressures	Yes, Increase
Assumed Variable Temperature of Liquid	Slower Condensation	No
Initial Bubble Radius	Collapse More Nearly Adiabatic	Pressure Similar at Similar Radius Ratio, but Larger Region is Affected for Larger Bubble
Thermal Conductivity of Contents	Some Reduction in Condensation Rates and Contents Temperature	Moderate Reduction
Liquid Overpressure	Higher Peak Pressure	Yes, Increase

REFERENCES

1. Mitchell, T.M., Hammitt, F.G., "Asymmetric Cavitation Bubble Collapse," to be published, ASME (1972).

2. Mitchell, R.M., "Numerical Studies of Asymmetric and Thermodynamic Effects on Cavitation Bubble Collapse," Ph.D. Thesis Dept. of Mech Engr., Univ. of Mich., Ann Arbor, Mich. December 1970; also available as ORA UMICH Rept. No. 03371-5-T.

3. Hickling, R., and Plesset, M., "Collapse and Rebound of a Spherical Bubble in Water," Phys. of Fluids, Vol. 7, No. 1 (1964).

4. Ivany, R.D., and Hammitt, F.G., "Cavitation Bubble Collapse in Viscous, Compressible Liquids -- Numerical Analysis," Trans. ASME, J. Basic Eng., 87 (1965), 977.

5. Zwick, S.A., and Plesset, M.S., "On the Dynamics of Small Vapor Bubbles in Liquids," J. Math. Phys., 33 (1955), 308-330.

6. Hickling, Robert, "I. Acoustic Radiation and Reflection from Spheres, II. Some Effects of Thermal Conduction and Compressibility in the Collapse of a Spherical Bubble in a Liquid," Ph.D. Thesis, Cal. Inst. Tech. (1962).

7. Florschuetz, L.W., and Chao, B.T., "On the Mechanics of Vapor Bubble Collapse," Trans. ASME, J. Heat Transfer, 87 (1965), 209-220.

8. Theofanous, T., Biasi, L., Isbin, H.S., and Fauske, H., "A Theoretical Study on Bubble Growth in Constant and Time-Dependent Pressure Fields," Chem. Eng. Sci., 24 (1969). 885-897.

9. Canavelis, R., "Contribution à l'Étude de l'Érosion de Cavitation dans les Turbomachines Hydrauliques," Thèses, La Faculté des Sciences de l'Université de Paris, France, Juin, 1966.

10. Scriven, L.E., "On the Dynamics of Phase Growth," Chem. Eng. Sci., 10 (1959), 1-13.

11. Poritsky, H., "The Collapse of Growth of a Spherical Bubble or Cavity in a Viscous Liquid," Proc. First National Congress of Appl. Mech., ASME, (1952) 813-821.

12. Kennard, E.H., Kinetic Theory of Gases, McGraw-Hill, New York, (1938), 68-70

13. Bornhorst, W.J., and Hatsopoulos, G.N., "Bubble - Growth Calculation without Neglect of Interfacial Discontinuities," Trans. ASME, J. Appl. Mech., 34, Series E (1967), 847-853.

14. Bornhorst, W.J., and Hatsopoulos, G.N., "Analysis of a Liquid Vapor Phase Change by the Methods of Irreversible Thermodynamics," Trans. ASME, J. Appl. Mech., 34, Series E (1967), 840-846.

15. Carslaw, H.S., and Jaeger, J.C., Conduction of Heat in Solids, Second Edition, Oxford University Press (1959), 233.

16. Theofanous, T.G., Biase, L., Isbin, H.S., and Fauske, H.K., "Nonequilibrium Bubble Collapse -- A Theoretical Study," AIChE Preprint 1, Presented at Eleventh National Heat Transfer Conference, Minneapolis, August, 1969.

17. Garcia, R., and Hammitt, F.G., "Cavitation Damage and Correlation with Material and Fluid Properties," Trans. ASME, J. Basic Eng., 89, Series D (1967), 753-763.

18. Hammitt, F.G., and Rogers, D.O., "Effects of Pressure and Temperature Variation in Vibratory Cavitation Damage Test," J. Mech. Eng. Sci, 12, 6, 1970, 432-439.

19. Kling, C.L., and Hammitt, F.G., "A Photographic Study of Spark-Induced Cavitation Bubble Collapse," (submitted for ASME presentation and publication), available as ORA UMICH 03371-4-T (Mod), Nov. 1971.

20. Florschuetz, L.W., and Al-Joubouri, "Generalized Quantitative Criteria for Predicting Rate-Controlling Mechanism for Vapor Bubble Growth in Superheated Liquids", Int. J. Heat Mass Transfer, 14, 587-600.